physics

MDPI

Article

Stabilizing Diamagnetic Levitation of a Graphene Flake through the Casimir Effect

Norio Inui

Graduate School of Engineering, University of Hyogo, Shosha 2167, Himeji 671-2201, Japan; inui@eng.u-hyogo.ac.jp

Abstract: Graphene exhibits diamagnetism, enabling it to be lifted by the repulsive force produced in an inhomogeneous magnetic field. However, the stable levitation of a graphene flake perpendicular to the magnetic field is impeded by its strong anisotropic of magnetic susceptibility that induces rotation. A method to suppress this rotation by applying the Casimir force to the graphene flake is presented in this paper. As a result, the graphene flake can archive stable levitation on a silicon plate when the gravitational force is small.

Keywords: Casimir effect; Casimir force; Casimir torce; diamagnetic levitation

1. Introduction

One of the promising applications of the Casimir effect [1,2] is the actuation of microelectromechanical systems (MEMS) [3–6]. Unlike conventional actuation methods that rely on electric power sources, the Casimir force, which arises from vacuum fluctuations, does not require an external energy source such as a battery. This advantage makes it a desirable option for MEMS actuation. However, the Casimir force can also lead to unexpected adhesion [7] between different parts of MEMS, causing their function to cease due to the omnipresence of vacuum fluctuations. To prevent this adhesion, a straightforward approach is to generate a repulsive force that levitates the MEMS parts. While the repulsive Casimir force [8] has been studied and observed in liquid environments [9], its utilization in atmospheric conditions has not been explored [10].

Levitating MEMS parts without them adhering to substrates can reduce friction and enhance the sensitivity sensors. Numerous methods for levitating objects in the atmosphere have been proposed, with magnetic levitation being a well-known technique. According to Earnshaw's theorem, the stable levitation of magnets cannot be achieved through a combination of static magnetic or gravitational force alone; additional control is required. However, the unique property of diamagnetism enables levitation in the atmosphere without the need for control [11,12].

Graphite, a highly diamagnetic material [13], can be stably levitated above neodymium magnets, and more recently, multi-layer graphene flakes have also been successfully levitated [14,15]. However, achieving stable levitation of a single-layer graphene flake above a magnet in an atmosphere setting remains an unmet challenge. When a magnetic field is applied perpendicularly to the surface of graphene, a strong magnetic moment is induced. In contrast, applying a magnetic field parallel to the surface results in minimal magnet moment induction. Consequently, the graphene rotates to align itself parallel to the magnetic field, leading to a loss of the levitation force.

This study investigates the levitation of a single graphene flake above a substrate, considering the interplay between the diamagnetic force and the Casimir force within the framework of the proximity force approximation (PFA) [16]. Normally, the Casimir force between a graphene sheet and a substrate is attractive, thereby reducing the levitation force. However, it is demonstrated that the Casimir effect can counteract rotation and enable the stable levitation of graphene.

Citation: Inui, N. Stabilizing Diamagnetic Levitation of a Graphene Flake through the Casimir Effect. *Physics* **2023**, *5*, 923–935. https://doi.org/10.3390/physics5030060

Received: 20 June 2023
Revised: 28 July 2023
Accepted: 7 August 2023
Published: 1 September 2023

For a configuration involving a small square plate and an infinitely large substrate arranged in parallel, the Casimir energy between them is negative and proportional to the area of the small plate. When the small plate tilts around an axis passing through its center and parallel to its sides, the projection area onto the substrate decreases due to the inclination. This decrease in the projection area contributes to an increase in the Casimir energy. Additionally, the distance between one side of the small plate and the substrate increases, further increasing the Casimir energy. However, the distance between the other side of the small plate and the substrate decreases, leading to a decrease in the Casimir energy. The stability of the parallel state relative to the substrate is determined by the summation of these contributions. For large separations, the last contribution is smaller than the others, resulting in a stable parallel state. If the torque induced by magnetic interaction can be canceled out by the Casimir effect, a graphene flake can be levitated stably in a vacuum.

The remainder of this paper is organized as follows: In Section 2, the magnetic properties of a graphene flake based on the tight-binding model is explained. Section 3 focuses on the levitation of a graphene flake, considering the balance between the force induced by a magnetic field and gravity. In Section 4, the approximation of the Casimir energy between a single-layer graphene and a silicon substrate as a summation of power functions is given. In Section 5, the change in the Casimir energy which is expressed as a power function, due to the rotation being is calculated. This also explores the relationship between the stability of the parallel state and the separation distance. In Section 6, the stability of a levitated graphene flake above a silicon substrate through the application of diamagnetic force is examined. In Section 7, the optimizing the applied magnetic field can lead to stabilization through the Casimir effect on Earth is demonstrated. Additionally, the calculation method beyond PFA is discussed. Finally, in the conclusion, the essential conditions required to achieve stable levitation are summarized.

2. Magnetic Properties of Graphene

The potential energy of a graphene flake in the presence of an external magnetic field is examined. In this study, the magnetic field is generated by passing an electric current through a coil. When the electric current is sufficiently large, the graphene flake can be levitated above the coil, as depicted in Figure 1a. The coil, with a radius R, is positioned above a silicon substrate at a separation distance d as illustrated in Figure 1b. It is important to note that the discussion focuses solely on the levitation achieved through the magnetic force, while the influence of the Casimir effect on the levitation is explored in subsequent Sections.

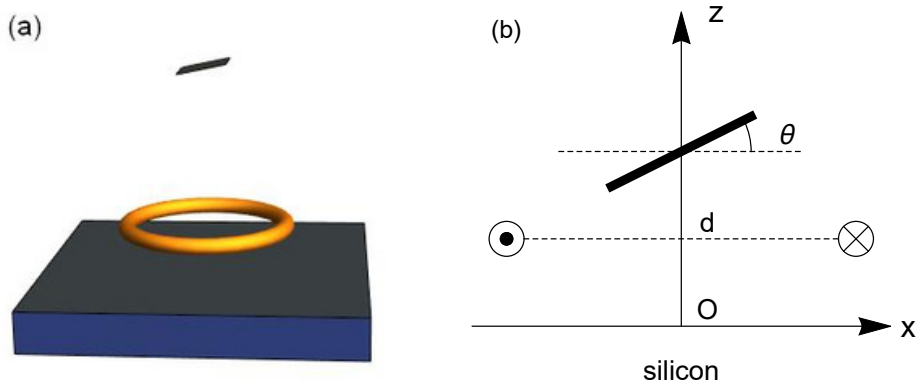

Figure 1. (**a**) Illustration of the levitation of a graphene flake in a magnetic field generated by an electric current flowing through a coil positioned above a silicon plate. (**b**) Positional relationship between the inclined graphene, coil, and silicon plate.

The magnetic flux density along the z-axis is expressed as follows:

$$B_z(z) = \frac{\mu_0 I R^2}{2[(z-d)^2 + R^2]^{3/2}}, \quad (1)$$

where I is the electric current through the coil, and $\mu_0 = 1.257 \times 10^{-6}$ NA^{-2} is the permeability in the vacuum. The direction of the electric current is counterclockwise when observed from above the ring. On the z-axis, the component of the magnetic flux density parallel to the substrate is zero.

The diamagnetic characteristics of graphene stem from the interaction between the induced electric current and the magnetic field. This study neglects the spin interactions and focus on the calculation of the energy eigenvalues of graphene, denoted as $\epsilon_i(B)$, which depend on the magnetic field. These eigenvalues are typically determined using the tight-binding model and the Peierls substitution method [17–19]. The Hamiltonian can be expressed as follows:

$$H = -\gamma_0 \sum_{\langle n,m \rangle} e^{i\phi_{nm}} \hat{c}_n^\dagger \hat{c}_m, \quad (2)$$

where γ_0 (=3 eV) is the transfer energy; $\hat{c}_n^\dagger$ and $\hat{c}_n$ are the annihilation and creation operators of an electron at site n, respectively. The magnetic dependence of the Hamiltonian is represented by Peierls phase, ϕ_{nm}, defined by

$$\phi_{nm} = \frac{e}{\hbar} \int_{\vec{r}_n}^{\vec{r}_m} d\vec{r} \cdot \vec{A}, \quad (3)$$

where $\vec{A}(r)$ is the vector potential, and $\vec{r}_s$ is the position of site s. The symbols e and $\hbar$ denote the elemantary charge and the reduced Planck constant, respectively. If the applied uniform magnetic field, B, is perpendicular to the graphene surface, the vector potential can be expressed by $(0, Bx, 0)$ in the Landau gauge.

By calculating eigenvalues $\epsilon_i(B)$ of the Hamiltonian, the free energy of graphene including the contribution from the orbital current induced by applying the magnetic field at temperature T is expressed as

$$\mathcal{F}_m(B) = -2k_B T \sum_i \ln\left[1 + \exp\left(\frac{\mu - \epsilon_i(B)}{k_B T}\right)\right], \quad (4)$$

where k_B and μ denote the Boltzmann constant and the chemical potential, respectively. In Equation (4), the factor of 2 is the spin degeneracy of the levels. The present sudy considers only the case of $\mu = 0$. When considering small magnetic fields, the induced magnetic moment of the graphene flake is directly proportional to the applied magnetic field. Consequently, the magnetic potential can be described as proportional to the inner product of the magnetic moment and the magnetic field. Thus, the magnetic potential for the small magnetic field is expressed as $c_m B^2$. The coefficient c_m depends on the size and edge type of graphene and is expressed as follows:

$$c_m = \frac{1}{2} \frac{\partial^2 \mathcal{F}_m(B)}{\partial B^2}\bigg|_{B=0}. \quad (5)$$

3. Levitation by Diamagnetic Force

In the case when the angle of inclination is zero and the change in the magnetic field within the graphene flake is disregarded, the total energy of the graphene system can be expressed as the sum of the magnetic energy and the gravitational energy:

$$U_{\mathrm{mg}}(z,d) = c_{\mathrm{m}}\frac{\mu_0^2 I^2 R^4}{4[(z-d)^2+R^2]^3} + mgz, \tag{6}$$

where m is the mass of graphene and g is gravitational acceleration. If d = 0 and the normalized position, $\zeta \equiv z/R$, is introduced, the total energy is expressed as

$$U_{\mathrm{mg}}(\zeta) = c_0\left[\frac{1}{(\zeta^2+1)^3} + \gamma\zeta\right], \tag{7}$$

where

$$c_0 = \frac{c_{\mathrm{m}}\mu_0^2 I^2}{4R^2}, \tag{8}$$

$$\gamma = \frac{mgR}{c_0}. \tag{9}$$

Figure 2a shows the dependence of U_{mg} on ζ for a different γ. For a small γ, there is a local minimum of U_{mg}, at which the magnetic force balances. Furthermore, this equilibrium point is stable. Thus, the graphene can be levitated stably along the z-axis. If $\gamma > \gamma_c \equiv 1.329$, no local minimum exists and the graphene falls to the substrate. Figure 2b shows the dimensionless levitation height, ζ_m, where U_{mg} takes a minimum valueas a function of γ. The dimensionless levitation height approaches 0.378 in the limit of $\gamma \to \gamma_c$.

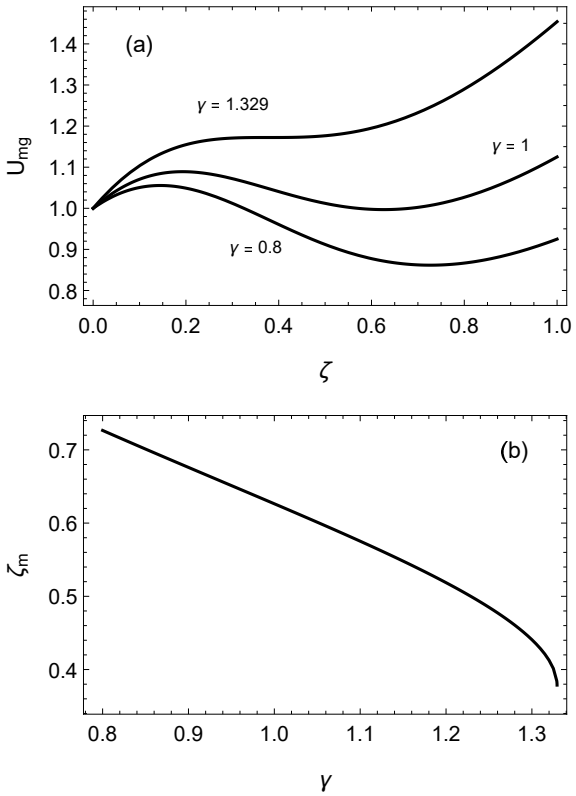

Figure 2. (**a**) The sum, U_{mg} (7), of magnetic and gravitational potential energies as a function of the nondimensional height, ζ, for different ratios, γ (9). (**b**) Relationship between the nondimensional levitation height, ζ_m, and γ.

The magnetic susceptibility of graphite vertical to the surface per mass, $\chi_\perp$, is -2.7×10^{-7} m^3/kg and one parallel to the surface per mass, $\chi_\parallel$, is -6.3×10^{-9} m^3/kg. Similarly, the orbital magnetic susceptibility of graphene when aligned parallel to the surface is expected to be significantly smaller than that when aligned perpendicularly to

the surface. Thus, it is assumed that $\chi_{\|}$ is zero in the following calculations. Accordingly, the magnetic energy of the inclined graphene with the angle θ of inclination is given by

$$U_{\rm m}(\zeta,\theta) = \frac{c_0\cos^2\theta}{(\zeta^2+1)^3}. \quad (10)$$

The gravitational energy of a graphene flake remains unaffected by its rotation. Consequently, the flake will rotate until it aligns as parallel to the magnetic field, causing the levitation force to diminish. As a result, the graphene flake descends and eventually comes in contact with the substrate.

4. Casimir Force between a Graphene Flake and a Silicon Plate

To address the issue of rotation, the utilization of the Casimir effect becomes crucial. According to the Lifshitz theory, the Casimir free energy per unit area between a single-layer graphene sheet and a dielectric plate, separated by a separation a and at a temperature T, can be expressed as the sum of contributions for different polarizations η of the electromagnetic field, namely transverse magnetic (TM) and transverse electric (TE):

$$\mathcal{F}_{\rm C}(a) = \mathcal{F}_{\rm TM}(a)+\mathcal{F}_{\rm TE}(a), \quad (11)$$

where

$$\mathcal{F}_{\eta}(a) = \frac{k_{\rm B}T}{8\pi a^2}{\sum_{l=0}^{\infty}}' \int_{\zeta_l}^{\infty} y dy \ln[1-r_{\eta}^{(g)}(i\zeta_l,y)r_{\eta}^{(p)}(i\zeta_l,y)e^{-y}]. \quad (12)$$

Here, ζ_l with nonnegative integer variable l is the dimensionless Matsubara frequencies defined by $4\pi a k_{\rm B}Tl/\hbar c$, with c denoting the speed of light, and $r_{\eta}^{(g)}$ and $r_{\eta}^{(p)}$ are the reflection coefficients on graphene and on a plate for the polarization η, respectively [20–25].

The reflection coefficients on a silicon plate are expressed as

$$r_{\rm TM}^{(p)}(i\zeta_l,y) = \frac{\epsilon_l y-\sqrt{y^2+\zeta_l^2(\epsilon_l-1)}}{\epsilon_l y+\sqrt{y^2+\zeta_l^2(\epsilon_l-1)},}, \quad (13)$$

$$r_{\rm TE}^{(p)}(i\zeta_l,y) = \frac{y-\sqrt{y^2+\zeta_l^2(\epsilon_l-1)}}{y+\sqrt{y^2+\zeta_l^2(\epsilon_l-1)}}, \quad (14)$$

where ϵ_l is the dielectric permittivity of silicon at the imaginary frequency, $2\pi i k_{\rm B}Tl/\hbar$, and calculated from the optical data [26] based on the Kramers–Kronig relation,

$$\epsilon(i\xi) = 1+\frac{2}{\pi}\int_0^{\infty}\frac{\omega {\rm Im}\epsilon(\omega)}{\omega^2+\xi^2}d\omega. \quad (15)$$

The reflection coefficients on graphene using the Dirac model are expressed as follows:

$$r_{\rm TM}^{(g)}(i\zeta_l,y) = \frac{y\Pi_{00}}{y\Pi_{00}+\frac{\hbar}{a}(y^2-\zeta_l^2)}, \quad (16)$$

$$r_{\rm TE}^{(g)}(i\zeta_l,y) = -\frac{(y^2-\zeta_l^2)\Pi_{\rm tr}-y^2\Pi_{00}}{(y^2-\zeta_l^2)(\Pi_{\rm tr}+\frac{\hbar}{a}y)-y^2\Pi_{00}}, \quad (17)$$

where Π_{00} is the 00-component of the polarization tensor, Π, and $\Pi_{\rm tr}=\Pi_1^1+\Pi_2^2$. The polarization tensor is determined by the temperature [27], mass gap parameter, δ_g, chemical potential, μ, and the Fermi velocity, $v_F = c/300$. The polarization tensor is described in detail in Ref. [21].

The circles in Figure 3 show the dependence of the Casimir energy per area between graphene with $\delta_g = \mu = 0$ and a silicon plate on the separation distance at temperature 300 K. The line represents a fitting function,

$$u_{\mathrm{C}}(z) = -\frac{c_3}{z^3} - \frac{c_2}{z^2}, \tag{18}$$

where $c_3 = 1.11 \times 10^{-12}$ Jm and $c_2 = 7.96 \times 10^{-11}$ J.

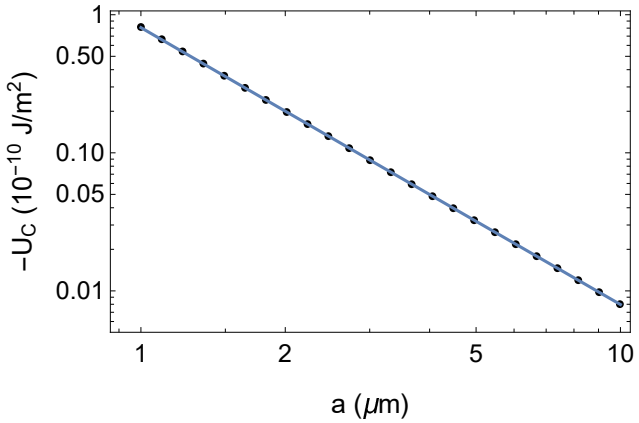

Figure 3. Casimir energy per area between a graphene sheet and a silicon plate calculated using the Lifshitz formula (circles) and the fitting function (line).

5. Change in the Casimir Energy by Inclining

The calculation of the Casimir energy between an inclined plate and a flat plate can be a computationally intensive task [28–30]. As an alternative approach, the PFA is employed. Within the PFA framework, the Casmir energy between an inclined square plate, with one side measuring $2L$, and an infinite substrate can be approximated by the following expression:

$$U_{\mathrm{C}}(a,\theta) = 2L\int_{-L\cos\theta}^{L\cos\theta} u[a-(\tan\theta)x]dx, \tag{19}$$

where $u(z)$ is the Casimir energy per area. If the Casimir energy per area obeys the power function, $u(z) = -c_\beta z^{-\beta}$, where c_β is a constant and $\beta > 1$, its dependence on θ is expressed as

$$U_{\mathrm{C}}(a,\theta,\beta) = -\frac{2c_\beta L}{(1-\beta)\tan\theta}\left[(a+L\sin\theta)^{1-\beta} - (a-L\sin\theta)^{1-\beta}\right]. \tag{20}$$

By introducing a dimensionless coordinate $\alpha \equiv a/L$, the normalized energy, $\tilde{U}$, with the absolute value at $\theta = 0$ is expressed as

$$\tilde{U}(\alpha,\theta,\beta) \equiv \frac{U(a,\theta,\beta)}{|U(a,0,\beta)|}, \tag{21}$$

$$= -\frac{\alpha^\beta}{2(1-\beta)}\frac{(\alpha+\sin\theta)^{1-\beta} - (\alpha-\sin\theta)^{1-\beta}}{\tan\theta}. \tag{22}$$

Figure 4a shows $\tilde{U}(\alpha,\theta,2)$ for $\alpha = 1.2$, $\sqrt{2}$, and 3. For the small values of α, representing small separation distances, a local minimum is present at the nonzero inclination angle and the flat state ($\theta = 0$) becomes unstable. As the separation increases above a threshold, $\alpha_c = \sqrt{2}$, the Casimir energy takes the minimum value at $\theta = 0$, and the flat state becomes stable. Figure 4b shows the relationship between the threshold α_c and exponent β. The thresholds α_c are 2 and $2\sqrt{5/3}$ for $\beta = 3$ and 4, respectively. A smaller exponent in the

Casimir energy equation enables the suppression of plate rotation to suppress from a smaller separation distance.

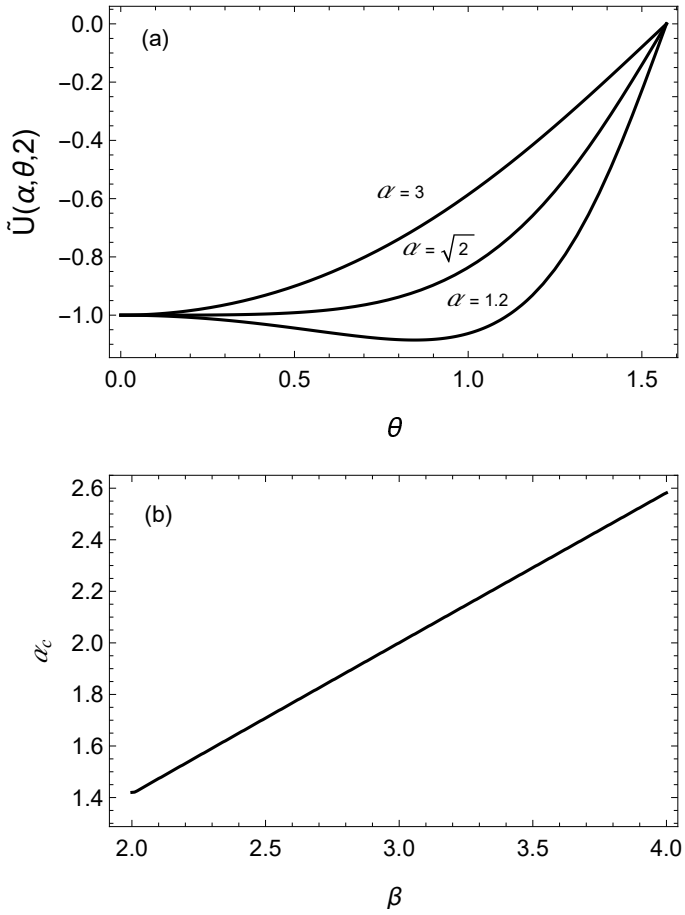

Figure 4. (**a**) Dependence of the potential energy, $U(\alpha, \theta, \beta = 2)$ (21), of an inclined plate on the angle, θ, of inclination for different dimensional heights, α. (**b**) Relationship between the threshold, α_c, above which the flat state is stable and the exponent, β, of the potential energy.

6. Levitation of a Graphene Flake above a Silicon Plate in a Magnetic Field

Let us proceed to investigate whether the suppression of rotation, discussed in Section 5, can contribute to stabilizing the levitation of a graphene flake in the presence of a magnetic field. If the graphene flake is levitated on a silicon plate, as depicted in Figure 1b, the total potential energy can be approximated given the following expression:

$$U(z,\theta) = U_{\mathrm{C}}(z,\theta,2) + U_{\mathrm{C}}(z,\theta,3) + U_{\mathrm{mg}}(z), \tag{23}$$

$$= -\frac{2c_2 L\cos\theta}{L^2\sin^2\theta - z^2} - \frac{2c_3 Lz\cos\theta}{(L^2\sin^2\theta - z^2)^2} + \frac{c_{\mathrm{m}}\mu_0^2 I^2 R^4}{4[(z-d)^2 + R^2]^3} + mgz, \tag{24}$$

where the Casimir energy between a graphene flake and a coil is neglected. Figure 5a shows the relationship between the total energy of a flat graphene flake and a silicon plate, and the separation distance, considering the gravitational acceleration g = 0 and 0.1 m/s^2. The parameters employed in the calculation are summarized in Table 1. Notably, one of the parameters, c_{m}, plays an important role in determining the magnetic force. Its value is specific to a graphene flake with hexagonal armchair edges at a temperature of 300 K (see Ref. [17] for details).

Table 1. Parameters used in the calculations. See text for details.

Parameters	Values
L	11.58 nm
R	4 μm
d	2.5 μm
I	0.3 A
c_{m}	1.24×10^{-5} eV/T^2
c_2	7.96×10^{-11} J
c_3	1.11×10^{-12} J m

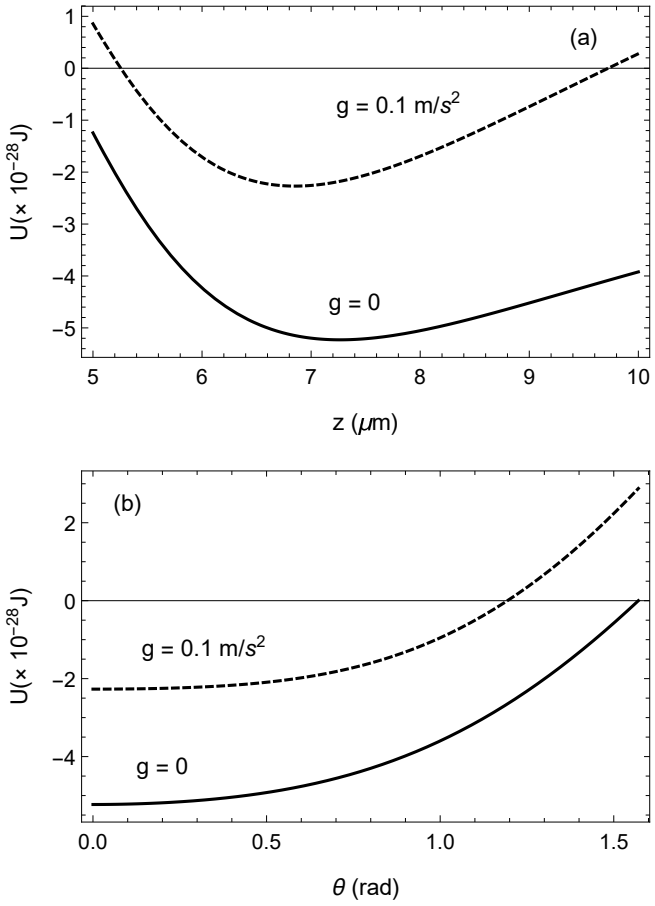

Figure 5. (**a**) Dependence of the total Casimir energy, magnetic energy, and gravitational energy on the separation distance for gravitational acceleration g = 0 and 0.1 m/s^2. (**b**) Dependence of the total energy at equilibrium heights on the inclined angle.

The levitation heights are measured to be 7.3 and 6.9 μm for the gravitational acceleration of 0 and 0.1 m/s^2, respectively. Figure 5b displays the change in the total energy due to inclination, with the minimum value of ΔU set to zero. The total energy monotonously increases as the graphene flake tilts away from θ = 0, indicating stable levitation when the gravitational acceleration is small. As the gravitational acceleration increases, the levitation height decreases. The results for g = 0.3 m/s^2 and 0.4 m/s^2 are presented in Figure 6a,b and illustrate the dependence of total energy on the position and inclination angle, respectively. When the graphene flake derivates from θ = 0, the total energy decreases, reaching its minimum at θ = 0.52 rad for g = 0.3 m/s^2. The inclined angle increases with an increase in gravitational acceleration. For g = 0.4 m/s^2, the angle of inclination, at which the total energy is minimized, is 0.67 rad. Figure 6c shows the total energy of inclined graphene flakes at θ = 0.52 rad for g = 0.3 and θ = 0.67 rad for g = 0.4 m/s^2. In the case of g = 0.3 m/s^2,

a local minimum exists in the total energy, enabling the levitation of the graphene flake in the inclined state. However, for g = 0.4 m/s^2, no local minimum exists, causing the graphene flake to fall onto the substrate after tilting.

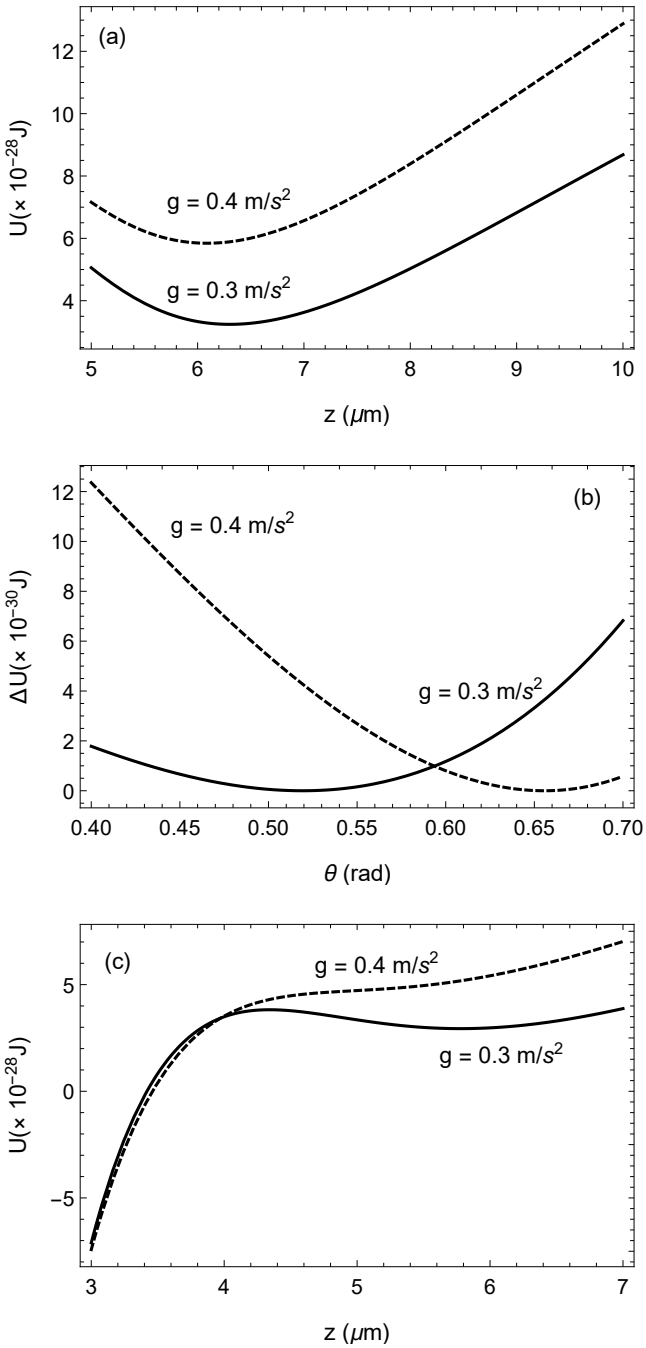

Figure 6. (**a**) Dependence of the total energy of the flat graphene flake for g = 0.4 and 0.3 m/s^2 on the vertical position. (**b**) Dependence of the total energy at equilibrium heights on the inclined angle for g = 0.4 and 0.3 m/s^2. The angle at which takes the minimum potential energy exists at non-zero inclined angle. (**c**) Dependence of the total energy of the graphene flakes that incline with the equilibrium angle on the separation distance.

7. Role of a Diamagnetic Force and the Casimir Torque

A diamagnetic force and the Casimir torque must be effectively combined to achieve stable levitation. In previous calculations, the magnetic field is generated by a circular current and the levitation was unsuccessful for large gravitational accelerations. However,

if an appropriate magnetic field is generated, then stable levitation can be realized. For example, when the magnetic flux density, which is expressed by $0.5 - 0.35\,z + 0.08z^2$ T, (where z is in μm) near $z = 2$ μm is generated, the total energy of the flat graphene flake for $g = 9.8$ m/s^2 takes a minimum at 2 μm as shown in Figure 7a. Furthermore, Figure 7b shows the total energy at the levitation height and takes the minimum in the flat state ($\theta = 0$), and indicates that stable levitation can be achieved on Earth if the appropriate magnetic field is generated.

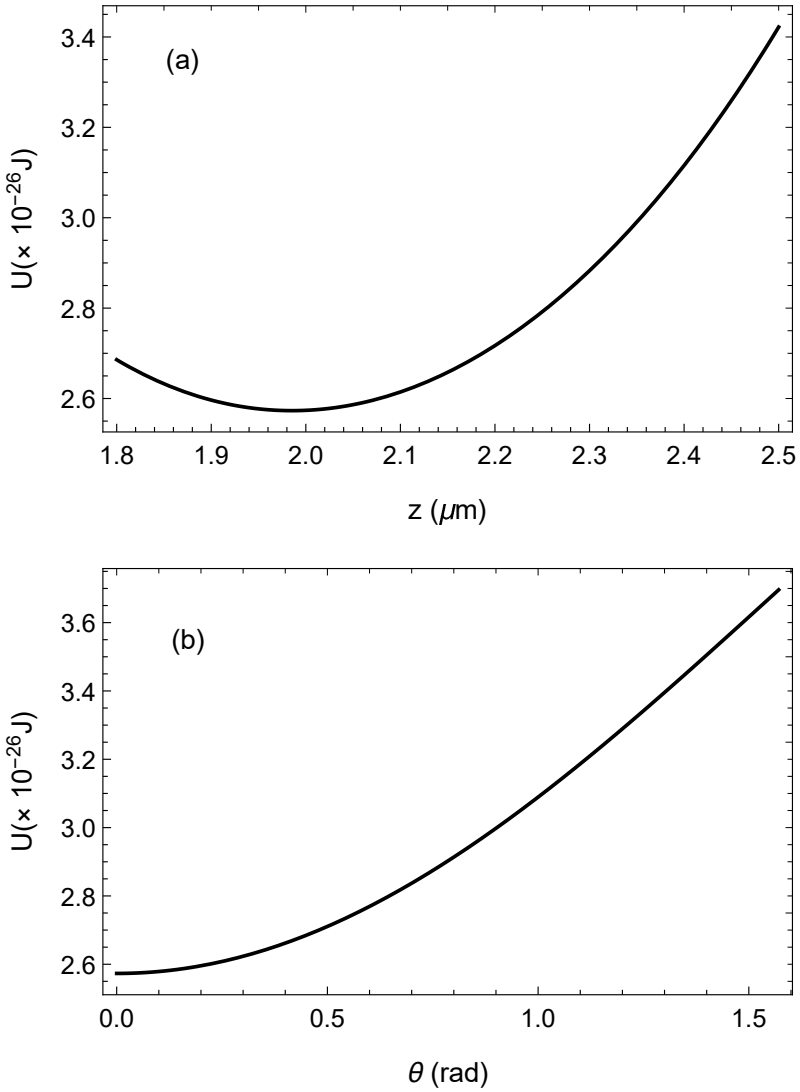

Figure 7. (**a**) Dependence of the total energy of the flat graphene flake for $g = 9.8$ m/s^2 on the vertical position. (**b**) Dependence of the total energy at equilibrium heights of 2 μm on the inclined angle for $g = 9.8$ m/s^2.

The stabilization of levitation results from the feature that the Casimir energy takes a minimum value when the plates are parallel for large separations. PFA worsens as the separation distance increases. However, the predicted stability of parallel configurations may be correct. For perfectly conductive plates, an analytical formula of the Casimir energy between non-parallel plates was presented in Ref. [30] using the optical approximation, which is one of the calculation methods beyond PFA [31–33]. Figure 8 shows the inclination angle of a square plate with side of size L above an infinite plate in a stable configuration, calculated using the optics approximation; θ^* is a function of the ratio of the separation distance between the square center and the infinite plate (δ). The parallel configuration with a zero inclination angle stabilizes when $\delta > 0.81$. Although sophisticated calculation

methods are necessary to determine the magnetic field accurately to realize levitation, the guideline indicating that stabilization through the Casimir effect is highly effective for large separations can be useful.

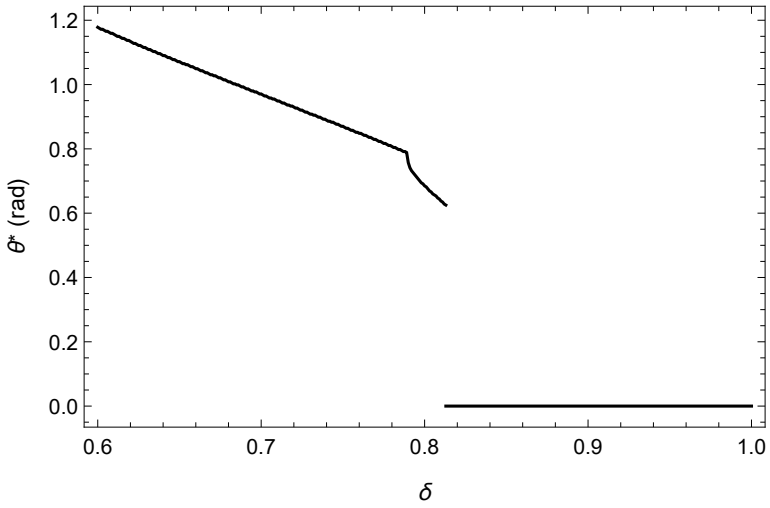

Figure 8. Dependence of the equilibrium of inclination angle, θ^*, obtained by the optical approximation on nomalized separation distance with the size of a plate, δ. The parallel configuration is stable for $\delta > 0.81$.

8. Conclusions

The coexistence of attractive and repulsive forces is crucial for achieving the levitation of objects. Furthermore, the behavior of these forces near the equilibrium point is of great importance. If they follow the power functions with the same exponent, the resulting function becomes monotonic, rendering stable levitation impossible.

The Casimir energy between objects is influenced by various physical parameters, such as the objects' shapes, distance between objects, permittivity, and temperature [27,34]. It is often represented by a power function. In the case of perfectly conductive plates, Casimir energy is inversely proportional to the cube of the separation distance, i.e., a^{-3}, regardless of the distance. However, if the permittivity is finite, Casimir energy varies as a^{-2} for small separations. This implies that the force between objects and its derivative can be manipulated by selecting appropriate materials and separation distances from an engineering perspective.

To counteract the rotation of the graphene flake and achieve stable levitation, a diamagnetic force was employed as a repulsive force. In order for the flake's surface to remain perpendicular to the magnetic field, it is necessary to fixate the surface and ensure that the product of the applied magnetic field and its derivative is sufficiently large. However, in a vacuum environment, the graphene flake tends to rotate, causing its surface to become parallel to the magnetic field. To address this issue, the Casimir torque was utilized as one of the methods for stabilization.

The numerical analysis revealed that the Casimir effect can provide some degree of stabilization for the diamagnetic levitation of a graphene flake. However, its effectiveness is limited, and it is insufficient to fully suppress the rotation in Earth's gravity by the magnetic field generated through the circular electric current. This limitation arises from the feature that the suppression of the rotation by the Casimir effect is most effective at larger separation distances. As the separation distance increases, the Casimir energy rapidly diminishes, resulting in a weaker restoring torque. Therefore, in order to achieve magnetic levitation in a strong gravitational field, furthering the optimization of the magnetic field is necessary as shown in Section 7.

As the separation distance approaches zero, the magnetic energy remains finite. However, the Casimir energy diverges to negative infinity. This implies that the levitation state

is metastable [35–37], and a potential barrier is present near the surface. The height of this potential barrier is not significant. Therefore, to maintain the levitation state, it is necessary to maintain a high vacuum and low temperature. These conditions help to stabilize the system and prevent the graphene flake from falling onto the substrate.

Funding: This research was funded by the Ministry of Education, Culture, Sports, Science and Technology, Grant-in-Aid for Scientific Research(C), MEXT KAKENHI, Japan, Grant Number 21K04895.

Data Availability Statement: Not applicable.

Conflicts of Interest: The author declares no conflicts of interest.

References

1. Milonni, P.W. *The Quantum Vacuum*; Academic Press, Inc.: San Diego, CA, USA, 1994. [CrossRef]
2. Bordag, M.; Klimchitskaya, G.L.; Mohideen, U.; Mostepanenko, V.M. *Advances in the Casimir Effect*; Oxford University Press: Oxford, UK, 2009. [CrossRef]
3. Chan, H.B.; Aksyuk, V.A.; Kleiman, R.N.; Bishop, D.J.; Capasso, F. Quantum mechanical actuation of microelectromechanical systems by the Casimir force. *Science* **2001**, *291*, 1941–1944. [CrossRef]
4. Capasso, F.; Munday, J.N.; Iannuzzi, D.; Chan, H.B. Casimir forces and quantum electrodynamical torques: Physics and nanomechanics. *IEEE J. Sel. Top. Quantum Electron.* **2007**, *13*, 400–414. [CrossRef]
5. Decca, R.; Aksyuk, V.; López, D. Casimir force in micro and nano electro mechanical systems. In *Casimir Physics*; Dalvit, D., Milonni, P., Roberts, D., da Rosa, F., Eds.; Springer: Berlin/Heidelberg, Germany, 2011; pp. 287–309. [CrossRef]
6. Zou, J.; Marcet, Z.; Rodriguez, A.W.; Reid, M.T.H.; McCauley, A.P.; Kravchenko, I.I.; Lu, T.; Bao, Y.; Johnson, S.G.; Chan, H.B. Casimir forces on a silicon micromechanical chip. *Nat. Commun.* **2013**, *4*, 1845. [CrossRef] [PubMed]
7. Palasantzas, G.; Sedighi, M.; Svetovoy, V.B. Applications of Casimir forces: Nanoscale actuation and adhesion. *Appl. Phys. Lett.* **2020**, *117*, 120501. [CrossRef]
8. Kenneth, O.; Klich, I.; Mann, A.; Revzen, M. Repulsive Casimir forces. *Phys. Rev. Lett.* **2002**, *89*, 033001. [CrossRef] [PubMed]
9. Munday, J.N.; Capasso, F.; Parsegian, V.A. Measured long-range repulsive Casimir–Lifshitz forces. *Nature* **2009**, *457*, 170–173. [CrossRef]
10. Kenneth, O.; Klich, I. Opposites attract: A theorem about the Casimir force. *Phys. Rev. Lett.* **2006**, *97*, 160401. [CrossRef]
11. Geim, A.K.; Simon, M.D.; Boamfa, M.I.; Heflinger, L.O. Magnet levitation at your fingertips. *Nature* **1999**, *400*, 323–324. [CrossRef]
12. Simon, M.D.; Geim, A.K. Diamagnetic levitation: Flying frogs and floating magnets (invited). *J. Appl. Phys.* **2000**, *87*, 6200–6204. [CrossRef]
13. McClure, J.W. Diamagnetism of graphite. *Phys. Rev.* **1956**, *104*, 666–671. [CrossRef]
14. Niu, C.; Lin, F.; Wang, Z.M.; Bao, J.; Hu, J. Graphene levitation and orientation control using a magnetic field. *J. Appl. Phys.* **2018**, *123*, 044302. [CrossRef]
15. Lin, F.; Niu, C.; Hu, J.; Wang, Z.; Bao, J. Graphene diamagnetism: Levitation, transport, rotation, and orientation alignment of graphene flakes in a magnetic field. *IEEE Nanotechnol. Mag.* **2020**, *14*, 14–22. [CrossRef]
16. Błocki, J.; Randrup, J.; Świątecki, W.J.; Tsang, C.F. Proximity forces. *Ann. Phys.* **1977**, *105*, 427–462. [CrossRef]
17. Ominato, Y.; Koshino, M. Orbital magnetism of graphene flakes. *Phys. Rev. B* **2013**, *87*, 115433. [CrossRef]
18. Espinosa-Ortega, T.; Luk'yanchuk, I.A.; Rubo, Y.G. Magnetic properties of graphene quantum dots. *Phys. Rev. B* **2013**, *87*, 205434. [CrossRef]
19. Deyo, S.; Hershfield, S. Magnetism in graphene flakes with edge disorder. *Phys. Rev. B* **2021**, *104*, 014404. [CrossRef]
20. Fialkovsky, I.V.; Marachevsky, V.M.; Vassilevich, D.M. Finite-temperature Casimir effect for graphene. *Phys. Rev. B* **2011**, *84*, 35446. [CrossRef]
21. Bordag, M.; Klimchitskaya, G.L.; Mostepanenko, V.M. Thermal Casimir effect in the interaction of graphene with dielectrics and metals. *Phys. Rev. B* **2012**, *86*, 165429. [CrossRef]
22. Klimchitskaya, G.L.; Mostepanenko, V.M. van der Waals and Casimir interactions between two graphene sheets. *Phys. Rev. B* **2013**, *87*, 75439. [CrossRef]
23. Banishev, A.A.; Wen, H.; Xu, J.; Kawakami, R.K.; Klimchitskaya, G.L.; Mostepanenko, V.M.; Mohideen, U. Measuring the Casimir force gradient from graphene on a SiO_2 substrate. *Phys. Rev. B* **2013**, *87*, 205433. [CrossRef]
24. Henkel, C.; Klimchitskaya, G.L.; Mostepanenko, V.M. Influence of the chemical potential on the Casimir-Polder interaction between an atom and gapped graphene or a graphene-coated substrate. *Phys. Rev. A* **2018**, *97*, 32504. [CrossRef]
25. Klimchitskaya, G.L.; Mostepanenko, V.M. Casimir and Casimir-Polder forces in graphene systems: Quantum field theoretical description and thermodynamics. *Universe* **2020**, *6*, 150. [CrossRef]
26. Palik, E.D. (Ed.) *Handbook of Optical Constants of Solids*; Academic Press, Inc.: San Diego, CA, USA, 1985; Volume 1. [CrossRef]
27. Liu, M.; Zhang, Y.; Klimchitskaya, G.L.; Mostepanenko, V.M.; Mohideen, U. Experimental and theoretical investigation of the thermal effect in the Casimir interaction from graphene. *Phys. Rev. B* **2021**, *104*, 085436. [CrossRef]
28. Mostepanenko, V.M.; Trunov, N.N. *The Casimir Effect and Its Applications*; Clarendon Press/Oxford University Press, Inc.: New York, NY, USA, 1997.

29. Scardicchio, A.; Jaffe, R.L. Casimir effects: An optical approach I. Foundations and examples. *Nucl. Phys. B* **2005**, *704*, 552–582. [CrossRef]
30. Guifoyle, B.; Klingenberg, W.; Sen, S. The Casimir effect between non-parallel plates by geometric optics. *Rev. Math. Phys.* **2005**, *17*, 859–880. [CrossRef]
31. Bordag, M.; Nikolaev, V. Casimir force for a sphere in front of a plane beyond proximity force approximation. *J. Phys. A* **2008**, *41*, 164002. [CrossRef]
32. Reynaud, S.; Maia Neto, P. A.; Lambrecht, A. Casimir energy and geometry: Beyond the proximity force approximation. *J. Phys. A* **2008**, *41*, 164004. [CrossRef]
33. Inui, N.; Kushiro, T.; Mochiji, K.; Moritani, M. Stable position of a micro torsion balance under the Casimir force. *e-J. Surf. Sci. Nanotech.* **2013**, *11*, 60–64. [CrossRef]
34. Sushkov, A.O.; Kim, W.J.; Dalvit, D.A.R.; Lamoreaux, S.K. Observation of the thermal Casimir force. *Nat. Phys.* **2011**, *7*, 230–233. [CrossRef]
35. Kramers, H.A. Brownian motion in a field of force and the diffusion model of chemical reactions. *Physica* **1940**, *7*, 284–304. [CrossRef]
36. Hanggi, P. Escape from a metastable state. *J. Stat. Phys.* **1986**, *42*, 105–148. [CrossRef]
37. Inui, N.; Maebuchi, K. Dynamic and fluctuation properties of a graphene disk levitated by a diamagnetic force in air. *J. Phys. D* **2022**, *55*, 285002. [CrossRef]